2019 American Control Conference (ACC)
Philadelphia, PA, USA, July 10-12, 2019

Exact and Approximate Stability Conditions for Cluster Synchronization of Kuramoto Oscillators

Tommaso Menara, Giacomo Baggio, Danielle S. Bassett, and Fabio Pasqualetti

***Abstract*— In this paper we derive exact and approximate conditions for the (local) stability of the cluster synchronization manifold for sparsely interconnected oscillators with heterogeneous and weighted Kuramoto dynamics. Cluster synchronization, which emerges when the oscillators can be partitioned in a way that their phases remain identical over time within each group, is critically important for normal and abnormal behaviors in technological and biological systems ranging from the power grid to the human brain. Yet, despite its importance, cluster synchronization has received limited attention, so that the fundamental mechanisms regulating cluster synchronization in important classes of oscillatory networks are still unknown. In this paper we provide the first conditions for the stability of the cluster synchronization manifold for general weighted networks of heterogeneous oscillators with Kuramoto dynamics. In particular, we discuss how existing results are inapplicable or insufficient to characterize the stability of cluster synchronization for oscillators with Kuramoto dynamics, provide rigorous quantitative conditions that reveal how the network weights and oscillators' natural frequencies regulate cluster synchronization, and offer examples to quantify the tightness of our conditions. Further, we develop approximate conditions that, despite their heuristic nature, are numerically shown to tightly capture the transition to stability of the cluster synchronization manifold.**

I. Introduction

Synchronization arises spontaneously and by design in a broad range of natural and man-made systems [1]–[3], and is characterized by the onset of coherent trajectories among different interconnected units. Full synchronization has been extensively studied, e.g., see [4], and it corresponds to the case where all of the units exhibit coherent behavior. In contrast and despite its fundamental importance for the functionalities of many network systems [5], cluster synchronization, where disjoint and, possibly, time-varying groups organize along different synchronized trajectories, has been the subject of fewer and isolated studies, e.g., see [6]–[8].

The underlying mechanisms of cluster synchronization are particularly useful to model, analyze, and regulate synchronized neural activity in the human brain (see Fig. 1). In fact, because different patterns of synchronized neural activity are thought to be clear biomarkers of different neurological disorders [9], [10], methods to characterize and control the large-scale structural architecture of the brain,

This material is based upon work supported in part by ARO 71603NSYIP, and in part by NSF BCS1631112. Tommaso Menara, Giacomo Baggio and Fabio Pasqualetti are with the Department of Mechanical Engineering, University of California at Riverside, {tomenara, gbaggio, fabiopas}@engr.ucr.edu. Danielle S. Bassett is with the Department of Bioengineering, the Department of Electrical and Systems Engineering, the Department of Physics and Astronomy, the Department of Psychiatry, and the Department of Neurology, University of Pennsylvania, dsb@seas.upenn.edu.

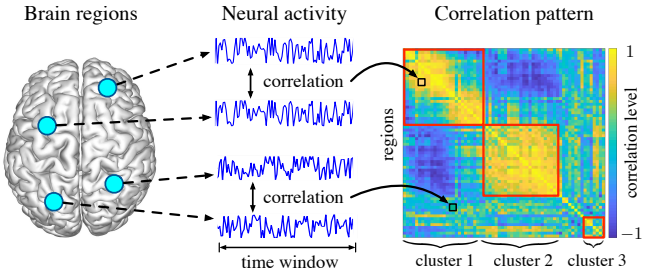

Fig. 1. As evident from fMRI scans, neural activity across different regions is correlated over time, and this correlation pattern defines clusters of synchronized brain areas corresponding to well-defined neural systems. Distinct correlation patterns are biomarkers of healthy and diseased neural states.

its intrinsic properties, and brain-wide oscillatory patterns, can inform the design of novel diagnostics and treatments for neurological diseases and psychiatric disorders. Motivated by these outstanding challenges, in this paper we derive prescriptive conditions for the stability of cluster synchronization in sparse networks of oscillators. We focus on oscillators with heterogeneous and weighted Kuramoto dynamics, which, despite their apparent simplicity, have been shown to be particularly suited to model the onset of complex synchronization phenomena in neural systems [11], as well as in many other natural and technological systems [1], [2].

Related work. Cluster synchronization is a challenging problem that has attracted the attention of the physics, dynamical systems, and controls communities. Existing studies on this topic have highlighted a relation between cluster synchronization and the presence of certain group symmetries [12], [13] and edge weights [6]–[8] in the underlying interconnection graph, for a class of coupled oscillators. Yet, as we show, group symmetries of the underlying graph are not necessary for cluster synchronization, and the Kuramoto model used in this paper does not satisfy the assumptions of the above papers, thus making the existing results inapplicable.

Cluster synchronization of oscillators with Kuramoto dynamics has been studied in [14], [15], where an approximate definition of cluster synchronization is used, in [16], [17], where conditions are given only for the *invariance* of the cluster synchronization manifold, in [18], where only the particular case of two clusters of identical Kuramoto oscillators with inertia is considered, and in [19], where only implicit and numerical stability conditions on the linearized dynamics are derived. To the best of our knowledge, this work presents the first conditions for the (local) stability of the cluster synchronization manifold in sparse and weighted networks of heterogeneous oscillators with Kuramoto dynamics.

978-1-5386-7926-5/$31.00 ©2019 AACC

Paper contribution. This paper makes two main contributions. First, we derive rigorous analytical conditions for the stability of the cluster synchronization manifold in weighted networks of Kuramoto oscillators. Specifically, (i) we leverage the theory of stability of perturbed nonlinear systems to derive quantitative conditions on the network weights that guarantee local exponential stability of the cluster synchronization manifold, and (ii) we develop a Lyapunov argument to show that, independent of the network weights, the cluster synchronization manifold becomes stable when the natural frequencies of the oscillators in disjoint clusters are sufficiently different (in their limit to infinity). These conditions reveal that the network weights and the oscillators' natural frequencies constitute two independent mechanisms to promote stability of the cluster synchronization manifold. Second, we derive approximate stability conditions by combining the low-pass behavior of the linearized dynamics of the isolated clusters with a small-gain result for interconnected time-varying systems. While relying on a heuristic argument, these approximate conditions involve both the aforementioned independent mechanisms, and are numerically shown to be considerably more accurate in predicting stability of the cluster synchronization manifold when compared to our exact conditions. Due to space constraints, proofs are omitted here and will be available in [20].

Mathematical notation. The sets $\mathbb{R}_{>0}$ and $\mathbb{R}_{\geq 0}$ denote the positive and nonnegative real numbers, respectively. The sets $\mathbb{S}^1$ and $\mathbb{T}^n$ denote the unit circle and the n-dimensional torus, respectively. The ℓ^2-norm is denoted as $\|\cdot\|$. A block-diagonal matrix is represented by $\mathrm{blkdiag}(\cdot)$. We denote a positive definite matrix A with $A \succ 0$. Let $\lambda_i(A)$ and $\sigma_i(A)$ denote the i-th eigenvalue and singular value of $A \in \mathbb{R}^{n\times n}$, respectively, and $\lambda_{\max}(A) = \max_i |\lambda_i(A)|$. Finally, let $\overline{\lambda}(A) = \frac{1}{n}\sum_i \lambda_i(A)$ and $\overline{\sigma}(A) = \frac{1}{n}\sum_i \sigma_i(A)$.

II. Problem Setup and Preliminary Notions

In this paper we characterize the stability properties of certain synchronized trajectories arising in networks of non-identical oscillators with Kuramoto dynamics. To this aim, let $\mathcal{G} = (\mathcal{V}, \mathcal{E})$ be the connected and weighted bidirected graph[1] representing the network of oscillators, where $\mathcal{V} = \{1, \dots, n\}$ and $\mathcal{E} \subseteq \mathcal{V}\times\mathcal{V}$ represent the oscillators, or nodes, and their interconnection edges, respectively. Let $A = [a_{ij}]$ be the weighted adjacency matrix of $\mathcal{G}$, where $a_{ij} \in \mathbb{R}_{>0}$ is the weight of the edge $(j,i) \in \mathcal{E}$, and $a_{ij} = 0$ when $(j,i) \notin \mathcal{E}$. The dynamics of the i-th oscillator reads as

$$\dot{\theta}_i = \omega_i + \sum_{j\neq i} a_{ij}\sin(\theta_j - \theta_i), \tag{1}$$

where $\omega_i \in \mathbb{R}_{>0}$ and $\theta_i \in \mathbb{S}^1$ denote the i-th oscillator's natural frequency and phase, respectively.

Let $\mathcal{P} = \{\mathcal{P}_1, \dots, \mathcal{P}_m\}$ be a nontrivial partition of $\mathcal{V}$, where each cluster contains at least two oscillators.[2] The network $\mathcal{G}$ exhibits cluster synchronization with partition $\mathcal{P}$ if the oscillators in each cluster evolve with equal phases. To be specific, we define the *cluster synchronization manifold* associated with the partition $\mathcal{P}$ as

$$\mathcal{S}_{\mathcal{P}} = \{\theta \in \mathbb{T}^n \ : \ \theta_i = \theta_j \text{ for all } i,j \in \mathcal{P}_k, k = 1,\dots,m\}.$$

Then, the network is cluster-synchronized with partition $\mathcal{P}$ when the phases of the oscillators belong to $\mathcal{S}_{\mathcal{P}}$ at all times.

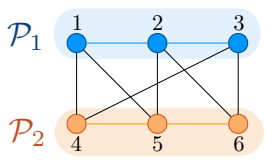

(a)

$$A = \left[\begin{array}{ccc|ccc} 0 & \alpha_1 & 0 & \beta_1 & \beta_2 & 0 \\ \alpha_1 & 0 & \alpha_2 & 0 & \beta_1 & \beta_2 \\ 0 & \alpha_2 & 0 & \beta_2 & 0 & \beta_1 \\ \hline \beta_1 & 0 & \beta_2 & 0 & \alpha_3 & 0 \\ \beta_2 & \beta_1 & 0 & \alpha_3 & 0 & \alpha_4 \\ 0 & \beta_2 & \beta_1 & 0 & \alpha_4 & 0 \end{array}\right]$$

(b)

Fig. 2. Fig. 2(a) illustrates a network of 6 oscillators with adjacency matrix as in Fig. 2(b). In this network, the partition $\mathcal{P} = \{\mathcal{P}_1, \mathcal{P}_2\}$, which satisfies Assumption (A2), cannot be identified by group symmetries of the network for any choice of the positive weights α_1, α_2, α_3, α_4, β_1 and β_2.

In this paper we characterize conditions on the network weights and the oscillators' natural frequency that guarantee *local exponential stability* of the cluster synchronization manifold $\mathcal{S}_{\mathcal{P}}$, for a given partition $\mathcal{P}$.[3] Because *invariance* of a set is a necessary condition for its stability [21, Chapter 3], we assume that $\mathcal{S}_{\mathcal{P}}$ is invariant under the oscillators' dynamics (1), or, equivalently [17], that the network of oscillators $\mathcal{G}$ satisfies the following conditions for the given partition $\mathcal{P}$:

(A1) The natural frequencies of the oscillators satisfy $\omega_i = \omega_j$ for every $i,j \in \mathcal{P}_k$ and $k \in \{1,\dots,m\}$;

(A2) The network weights satisfy $\sum_{k\in\mathcal{P}_\ell} a_{ik} - a_{jk} = 0$ for every $i,j \in \mathcal{P}_z$ and $z,\ell \in \{1,\dots,m\}$, with $z \neq \ell$.

Remark 1: ***(Network symmetries and balanced weights)*** Several conditions ensuring invariance and stability of $\mathcal{S}_{\mathcal{P}}$ require the network to satisfy restrictive group symmetries, e.g., see [12], [19]. As shown in Fig. 2, cluster synchronization does not require symmetric networks. Thus, the stability conditions derived in this work apply to a larger set of networks, and in fact different dynamics, compared to existing results on cluster synchronization. □

Define the phase difference $x_{ij} = \theta_j - \theta_i$, and notice that

$$\dot{x}_{ij} = \omega_j - \omega_i + \sum_{z=1}^{n} a_{jz}\sin(x_{jz}) - a_{iz}\sin(x_{iz}). \tag{2}$$

Further, define the following undirected graphs (see Fig. 3):

(i) the graph of the k-th cluster $\mathcal{G}_k = (\mathcal{P}_k, \mathcal{E}_k)$, where $\mathcal{E}_k = \{(i,j) : (i,j) \in \mathcal{E},\ i,j \in \mathcal{P}_k\}$;

(ii) a spanning tree $\mathcal{T}_k = (\mathcal{P}_k, \mathcal{E}_{\text{span},k})$ of $\mathcal{G}_k$;[4]

(iii) a spanning tree $\mathcal{T} = (\mathcal{V}, \mathcal{E}_{\mathcal{T}})$ of $\mathcal{G}$ with $\mathcal{E}_{\mathcal{T}} = \bigcup_{k=1}^m \mathcal{E}_{\text{span},k} \cup \mathcal{E}_{\text{inter}}$, where $|\mathcal{E}_{\text{inter}}| = m-1$.

Finally, define the following vectors of phase differences:

(iv) $x_{\text{intra}}^{(k)} = [x_{ij}]$, for all $(i,j) \in \mathcal{E}_{\text{span},k}$ with $i < j$,

(v) $x_{\text{intra}} = \left[x_{\text{intra}}^{(1)\mathsf{T}}, \dots, x_{\text{intra}}^{(m)\mathsf{T}}\right]^{\mathsf{T}}$, and

[1] A bidirected graph is a directed graph where $(i,j) \in \mathcal{E}$ implies $(j,i) \in \mathcal{E}$. The adjacency matrix of a bidirected graph needs not be symmetric.

[2] The case $m = 1$ leads to full synchronization, and it is not studied here.

[3] Loosely speaking, the manifold $\mathcal{S}_{\mathcal{P}}$ is locally exponentially stable if θ converges to $\mathcal{S}_{\mathcal{P}}$ exponentially fast when $\theta(0)$ is sufficiently close to $\mathcal{S}_{\mathcal{P}}$.

[4] We assume that the subgraphs $\mathcal{G}_k$ of $\mathcal{G}$ are connected. This guarantees the existence of the undirected spanning trees in (ii) and (iii).

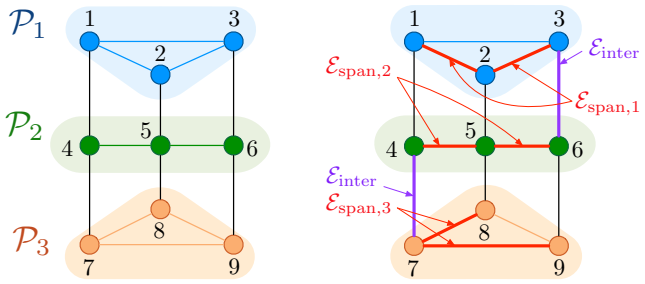

(a) (b)

Fig. 3. This figure illustrates the graph-theoretic definitions introduced in Section II for a network of 9 Kuramoto oscillators. Fig. 3(a) shows the partitions $\mathcal{P} = \{\mathcal{P}_1, \mathcal{P}_2, \mathcal{P}_3\}$, where $\mathcal{P}_1 = \{1, 2, 3\}$, $\mathcal{P}_2 = \{4, 5, 6\}$ and $\mathcal{P}_3 = \{7, 8, 9\}$. In Fig. 3(b), $\mathcal{E}_{\text{span},1}$, $\mathcal{E}_{\text{span},2}$, and $\mathcal{E}_{\text{span},3}$ represent (in red) the edges of the intra-cluster spanning trees $\mathcal{T}_1$, $\mathcal{T}_2$ and $\mathcal{T}_3$, while the edges belonging to the set $\mathcal{E}_{\text{inter}}$ are depicted in purple. The vectors of intra-cluster differences read as $x^{(1)}_{\text{intra}} = [x_{12}\ x_{23}]^\mathsf{T}$, $x^{(2)}_{\text{intra}} = [x_{45}\ x_{56}]^\mathsf{T}$, and $x^{(3)}_{\text{intra}} = [x_{78}\ x_{79}]^\mathsf{T}$, and the inter-cluster differences read as $x_{\text{inter}} = [x_{36}\ x_{47}]^\mathsf{T}$.

(vi) $x_{\text{inter}} = [x_{ij}]$, for all $(i,j) \in \mathcal{E}_{\text{inter}}$ with $i < j$.

It should be noticed (see also Fig. 3) that the vectors $x^{(k)}_{\text{intra}}$, x_{intra} and x_{inter} contain, respectively, $n_{\text{intra},k} = |\mathcal{P}_k| - 1$, $n_{\text{intra}} = n - m$ and $n_{\text{inter}} = m - 1$ entries. Notice also that every phase difference can be computed as a linear function of x_{intra} and x_{inter}. To see this, let $i, j \in \mathcal{V}$, and let $\mathrm{p}(i,j) = \{p_1, \dots, p_\ell\}$ be the unique path on $\mathcal{T}$ from i to j. Define $\mathrm{diff}(\mathrm{p}(i,j)) = \sum_{k=1}^{\ell-1} s_k$, where $s_k = x_{p_k p_{k+1}}$ if $p_k < p_{k+1}$, and $s_k = -x_{p_{k+1} p_k}$ otherwise. Then, $x_{ij} = \mathrm{diff}(\mathrm{p}(i,j))$, and the vectors x_{intra} and x_{inter} contain a smallest set of phase differences that can be used to quantify synchronization among all of the oscillators in the network.

In the remaining part of this section we rewrite the intra-cluster dynamics in a form that will be useful to present our results. In particular, for $(i,j) \in \mathcal{E}_{\text{span},k}$, the dynamics (2) of the intra-cluster difference x_{ij} can be rewritten as

$$\dot{x}_{ij} = \underbrace{\sum_{z \in \mathcal{P}_k} a_{jz} \sin(\mathrm{diff}(\mathrm{p}(j,z))) - a_{iz} \sin(\mathrm{diff}(\mathrm{p}(i,z)))}_{F^{(k)}_{ij}(x^{(k)}_{\text{intra}})} + \underbrace{\sum_{z \notin \mathcal{P}_k} a_{jz} \sin(\mathrm{diff}(\mathrm{p}(j,z))) - a_{iz} \sin(\mathrm{diff}(\mathrm{p}(i,z)))}_{G^{(k)}_{ij}(x_{\text{intra}}, x_{\text{inter}})},$$

which leads to

$$\dot{x}^{(k)}_{\text{intra}} = F^{(k)}(x^{(k)}_{\text{intra}}) + G^{(k)}(x_{\text{intra}}, x_{\text{inter}}), \tag{3}$$

where $F^{(k)}$ is the vector of $F^{(k)}_{ij}$ and $G^{(k)}$ is the vector of $G^{(k)}_{ij}$, for all $(i,j) \in \mathcal{E}_{\text{span},k}$, $i < j$. Finally, by concatenating the dynamics of $x^{(k)}_{\text{intra}}$ for all $k = 1, \dots, m$, we obtain

$$\dot{x}_{\text{intra}} = F(x_{\text{intra}}) + G(x_{\text{intra}}, x_{\text{inter}}). \tag{4}$$

Let $\mathcal{C}$ be the set of connected pairs of clusters; that is, $\mathcal{C} = \{(\ell, z) \ : \ \exists\ (i,j) \in \mathcal{E}$ with $i \in \mathcal{P}_\ell, j \in \mathcal{P}_z$, and $\ell < z\}$. Let x_{nom} denote the trajectory x_{inter} when $x_{\text{intra}} = 0$ at all times, and notice that $x_{ij} = x^{(\ell z)}$ for any $i \in \mathcal{P}_\ell$ and $j \in \mathcal{P}_z$ with $(\ell, z) \in \mathcal{C}$. Then, the linearization of the intra-cluster dynamics (4) around the trajectory $x_{\text{intra}} = 0$ and $x_{\text{inter}} = x_{\text{nom}}$ reads as follows:

$$\dot{x}_{\text{intra}} = (J_{\text{intra}} + J_{\text{inter}})\, x_{\text{intra}}, \tag{5}$$

where the matrices J_{intra} and J_{inter} are defined as

$$J_{\text{intra}} = \left.\frac{\partial F(x_{\text{intra}})}{\partial x_{\text{intra}}}\right|_{x_{\text{intra}}=0} = \mathrm{blkdiag}\,(J_1, \dots, J_m), \tag{6}$$

$$J_{\text{inter}} = \left.\frac{\partial G}{\partial x_{\text{intra}}}\right|_{\substack{x_{\text{intra}}=0 \\ x_{\text{inter}}=x_{\text{nom}}}} = \sum_{(\ell,z)\in\mathcal{C}} \cos\left(x^{(\ell z)}\right) J^{(\ell z)}_{\text{inter}}. \tag{7}$$

In other words, the linearization of the intra-cluster dynamics (4) along cluster-synchronized trajectories yields a time-varying system due to (7). This marks an important difference between cluster and full synchronization, where the dynamics in proximity of the synchronization manifold are time-invariant, and calls for novel and more involved conditions for cluster synchronization.

III. Exact Stability Conditions for Cluster Synchronization

In this section we derive sufficient stability conditions for local exponential stability of the cluster synchronization manifold. We make the following assumption,

(A3) The matrix J_{intra} in (6) is Hurwitz stable,

which can be shown to be satisfied, for instance, in the case of symmetric network weights ($A = A^\mathsf{T}$) [4], [20]. Our first stability result leverages tools from perturbation theory [22, Chapter 9] and the following instrumental lemma.

Lemma 3.1: ***(Bounded norm of inter-cluster dynamics)*** Let $G^{(k)}(x_{\text{intra}}, x_{\text{inter}})$ be as in (3), $\kappa = 2 \max_r n_{\text{intra},r}$, and

$$\gamma^{(k\ell)} = \begin{cases} \kappa \displaystyle\sum_{j \in \mathcal{P}_\ell} a_{ij}, & \text{if } \ell \neq k, \\ \kappa \displaystyle\sum_{\ell \neq k} \sum_{j \in \mathcal{P}_\ell} a_{ij}, & \text{otherwise,} \end{cases} \tag{8}$$

with $k, \ell \in \{1, \dots, m\}$ and $i \in \mathcal{P}_k$. Then,

$$\|G^{(k)}(x_{\text{intra}}, x_{\text{inter}})\| \leq \sum_{\ell=1}^{m} \gamma^{(k\ell)} \|x^{(\ell)}_{\text{intra}}\|.$$

As formalized in the next theorem, Lemma 3.1 states that the inter-cluster dynamics are linearly bounded and, together with results on stability of perturbed systems, implies that the origin of (4), and thus the cluster synchronization manifold $\mathcal{S}_\mathcal{P}$, is exponentially stable for some choices of the network weights. Recall that an M-matrix is a real nonsingular matrix $A = [a_{ij}]$ such that $a_{ij} \leq 0$ for all $i \neq j$ and all leading principal minors are positive [23, Chapter 2.5].

Theorem 3.2: ***(Sufficient condition on network weights for the stability of $\mathcal{S}_\mathcal{P}$)*** Let $\gamma^{(k\ell)}$ be the constants defined in (8), and define the matrix $S \in \mathbb{R}^{m \times m}$ as

$$S = [s_{k\ell}] = \begin{cases} \lambda^{-1}_{\max}(X_k) - \gamma^{(kk)} & \text{if } k = \ell, \\ -\gamma^{(k\ell)} & \text{if } k \neq \ell, \end{cases} \tag{9}$$

where $X_k \succ 0$ satisfies $J_k^\mathsf{T} X_k + X_k J_k = -I$ with J_k as in (6). If S is an M-matrix, then the cluster synchronization manifold is locally exponentially stable.

Theorem 3.2 contains a sufficient condition on the network weights for the stability of the cluster synchronization manifold $\mathcal{S}_\mathcal{P}$. Qualitatively, Theorem 3.2 proves that $\mathcal{S}_\mathcal{P}$ is locally exponentially stable when the intra-cluster coupling (measured by $\lambda_{\max}^{-1}(X_k)$) is sufficiently stronger than the perturbation induced by the inter-cluster connections (quantified by $\gamma^{(k\ell)}$). Quantitatively, as illustrated in Fig. 4(c), the condition in Theorem 3.2 is often conservative, possibly because it does not account for the contribution of the oscillators' natural frequencies to promote synchronization.

Theorem 3.3: ***(Stability of $\mathcal{S}_\mathcal{P}$ for large natural frequency differences)*** Let ω_i be the natural frequency of the oscillators in the i-th cluster, with $i \in \{1,\dots,m\}$. In the limit $|\omega_i - \omega_j| \to \infty$ for all $i,j \in \{1,\dots,m\}$, the cluster synchronization manifold is locally exponentially stable.

Theorem 3.3 proves that the cluster synchronization manifold is stable in the limit of infinitely different natural frequencies across the clusters. Some comments are in order. First, although Theorem 3.3 contains an asymptotic result, Fig. 4(d) and our analysis in Section IV show that heterogeneous yet bounded natural frequencies are sufficient to guarantee stability of the cluster synchronization manifold. Second, Theorems 3.2 and 3.3 prove that cluster synchronization can be achieved through two independent mechanisms that rely, respectively, on the network weights and on the oscillators' natural frequencies. Tighter stability conditions are expected to arise from the combination of these independent stability mechanisms, as we successfully pursue in the next section.

Example 1: ***(Comparison between stability conditions)*** Consider the network in Fig. 4(a) with partition $\mathcal{P} = \{\mathcal{P}_1,\mathcal{P}_2\}$, where $\mathcal{P}_1 = \{1,2\}$ and $\mathcal{P}_2 = \{3,4\}$, and adjacency matrix as in Fig. 4(b). The parameters $\alpha_1,\alpha_2 \in \mathbb{R}_{>0}$ and $\beta \in \mathbb{R}_{>0}$ denote the intra- and inter-cluster couplings, respectively. The matrix S in Theorem 3.2 becomes $S = \begin{bmatrix} 4\alpha_1-2\beta & -2\beta \\ -2\beta & 4\alpha_2-2\beta \end{bmatrix}$. In Fig. 4(c) we compare stability conditions based on the matrix S in (9) and numerical conditions given by Floquet stability theory.[5] Notice that, for certain parameters, the synchronization manifold is unstable. Finally, Fig. 4(d) shows that, as the inter-cluster coupling β grows, the stability of $\mathcal{S}_\mathcal{P}$ is achieved by increasing the difference of the natural frequencies, as predicted by Theorem 3.3. □

IV. Approximate Stability Conditions for Cluster Synchronization

Stability of cluster synchronization is guaranteed by the stability of the time-varying *interconnected* system (5), where the subsystems are identified by the isolated clusters. For interconnected systems with time-varying dynamics

$$\dot{y}_i = A_i(t)y_i + \sum_{j\neq i} B_{ij}(t)y_j, \quad i = 1,\dots,m, \tag{10}$$

where $A_i(t)$ and $B_{ij}(t)$ are time-varying matrices of suitable dimensions, a simplified version of the small-gain theorem can readily be derived from [25] and reads as follows.

[5]This comparison is possible for the case of two clusters, as we are able to explicitly derive the trajectory of the periodic inter-cluster difference [20].

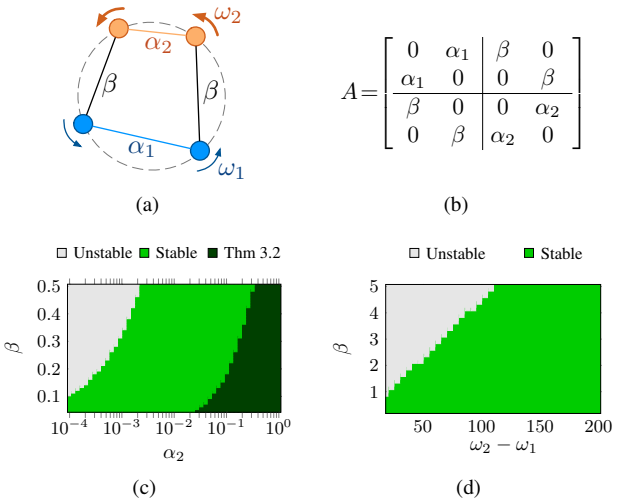

Fig. 4. Fig. 4(a) illustrates the network of 4 Kuramoto oscillators in Example 1. We identify the clusters $\mathcal{P}_1$ and $\mathcal{P}_2$ in blue and orange, respectively. Fig. 4(c) compares the stability conditions of Theorem 3.2 and numerical stability via Floquet decomposition [24]. We fix $\alpha_1 = \omega_1 = 1$, $\omega_2 = 8$, and let α_2 and β vary. The condition in Theorem 3.2 (dark green) identifies a subset of the stable configurations (light green). Fig. 4(d) illustrates that stability is guaranteed for sufficiently heterogeneous natural frequencies, as predicted by Theorem 3.3 ($\alpha_1 = \omega_1 = 1$, $\alpha_2 = 0.001$).

Theorem 4.1: ***(Small-gain stability test [25])*** The origin of the system in (10) is (globally) exponentially stable if:

(i) the origin of each isolated subsystem $\dot{y}_i = A_i(t)y_i$ is (globally) exponentially stable;

(ii) there exist $\xi_{ij} \in \mathbb{R}_{\geq 0}$ (*gains*) s.t., $\forall\, t \geq 0$, $\|y_{i,f}(t)\| \leq \sum_{j\neq i} \xi_{ij} \sup_{\tau\in[0,t]} \|y_j(\tau)\|$, $i = 1,\dots,m$, where $y_{i,f}(t)$ is the forced response of the i-th subsystem;

(iii) the matrix $\Xi \triangleq [\xi_{ij}] \in \mathbb{R}^{m\times m}$ (*gain matrix*) satisfies

$$\lambda_{\max}(\Xi) < 1. \tag{11}$$

As conditions (i)-(ii) in Theorem 4.1 are generally difficult to verify in systems with time-varying dynamics, in what follows we propose and validate an approximation to the dynamics (5), which allows us to apply Theorem 4.1 and derive (approximate) stability conditions for the cluster synchronization manifold. As we will show through numerical examples, our approximate stability conditions are tight.

To simplify the derivation of our approximate stability conditions, we start with the case of clusters with two nodes, so that the dynamics of the intra-cluster phase difference is scalar. This procedure extends directly to the general case. To obtain our stability condition, we follow three main steps.

(Approximate input-output response of the system (5)*)* The scalar intra-cluster dynamics of the k-th cluster reads as

$$\dot{x}^{(k)}_{\text{intra}} = (J_k + J_{\text{inter},k})x^{(k)}_{\text{intra}} + \sum_{\ell\neq k} J_{\text{inter},k\ell}\, x^{(\ell)}_{\text{intra}}, \tag{12}$$

where J_k, $J_{\text{inter},k} = \sum_{\ell\neq k} \eta_{k\ell}\cos(x^{(k\ell)})$, $J_{\text{inter},\ell z} = \zeta_{\ell z}\cos(x^{(\ell z)})$, $\eta_{k\ell}$, and $\zeta_{\ell z}$ are scalar quantities derived from (5). As $\omega^{(\ell z)} \triangleq \omega_z - \omega_\ell$ grows, we have [6] $x^{(\ell z)}(t) \approx$

[6]This approximation is reasonable for heterogeneous natural frequencies [20, Lemma A.2]. The same approximation has been used also in [14], although for a different analysis of cluster synchronization.

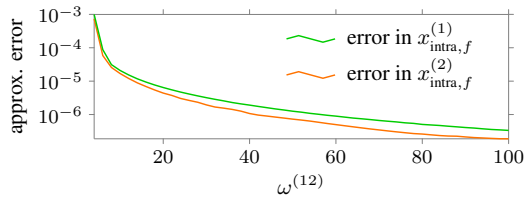

Fig. 5. In this figure we plot the maximum error between the forced response of (12) and the proposed approximation in (13) as $\omega^{(12)}$ increases. For the simulation, $\alpha_1 = \beta_1 = \omega_1 = 1$, $\alpha_2 = 0.01$, and ω_2 varies as indicated. Initial conditions are chosen randomly in the interval $(0, 0.001]$.

$\omega^{(\ell z)}t$. Thus, $J_{\text{inter},k} \approx \sum_{\ell \neq k} \eta_{k\ell} \cos(\omega^{(k\ell)}t)$, $J_{\text{inter},\ell z} \approx \zeta_{\ell z} \cos(\omega^{(\ell z)}t)$, and the approximate forced response of (12) to the input $x^{(\ell)}_{\text{intra}}$ becomes

$$x^{(k)}_{\text{intra},f} \approx \sum_{\ell \neq k} \int_0^t e^{J_k(t-\tau)} \zeta_{k\ell} \cos(\omega^{(k\ell)}\tau) x^{(\ell)}_{\text{intra}}(\tau)\, \mathrm{d}\tau, \quad (13)$$

where we have approximated the transition matrix of the linear time-varying system (12) as (see also [24]) $e^{\int_0^t J_k + J_{\text{inter},k}\mathrm{d}\tau} \approx e^{\int_0^t J_k \mathrm{d}\tau} = e^{J_k t}$. The last approximation is motivated by the fact that $J_{\text{inter},k}$ is a high-frequency signal with zero mean, so that its integral over time becomes negligible compared to the integral of J_k. Our approximation is validated in Fig. 5 for the network in Fig. 4(a), where we see that the input-output responses of the original (12) and approximated (13) systems remain close to each other for different values of the natural frequency.

(Computation of approximate input-output gains) Equation (13) can be viewed as the forced response of a linear time-invariant system with matrix J_k to the modulated input $\zeta_{k\ell}\cos(\omega^{(k\ell)}\tau)x^{(\ell)}_{\text{intra}}$. Following [26], each term in the sum in (13) can be expressed as a Taylor series about the natural frequency of the modulating function. This yields

$$x^{(k)}_{\text{intra},f}(t) = \sum_{\ell \neq k} \zeta_{k\ell} \underbrace{\sum_{r=0}^{\infty} c_r^{(k\ell)} \cos(\omega^{(k\ell)}t + \psi_r^{(k\ell)}) \frac{\mathrm{d}^r x^{(\ell)}_{\text{intra}}(t)}{\mathrm{d}t^r}}_{C_{k\ell}} \quad (14)$$

with $H_k(s) \triangleq \frac{1}{s - J_k}$, $c_r^{(k\ell)} = \left| \frac{\mathrm{i}^{-r}}{r!} \frac{\mathrm{d}^r H_k(\mathrm{i}\,\omega)}{\mathrm{d}\omega^r}\Big|_{\omega=\omega^{(k\ell)}} \right|$, and $\psi_r^{(k\ell)} = \text{angle}\left(\frac{\mathrm{i}^{-r}}{r!} \frac{\mathrm{d}^r H_k(\mathrm{i}\,\omega)}{\mathrm{d}\omega^r}\Big|_{\omega=\omega^{(k\ell)}} \right)$.

We propose the following first-order approximation of (14):

$$|C_{k\ell}| \approx \begin{cases} |H_k(\mathrm{i}\,\omega^{(k\ell)})|\ |x^{(\ell)}_{\text{intra}}(t)|, & \text{if } J_k \leq J_\ell, \\ \frac{|H_k(0)|}{|H_\ell(0)|} |H_\ell(\mathrm{i}\,\omega^{(k\ell)})|\ |x^{(\ell)}_{\text{intra}}(t)|, & \text{if } J_\ell < J_k. \end{cases} \quad (15)$$

Loosely speaking, the former approximation is motivated by the fact that the modulated input coming from the ℓ-th system is "slower" than the k-th system. Instead, the second approximation is valid when the input from the ℓ-th system is "faster" than the k-th system, and it follows from [26]. Using (15), we define the approximate input-ouput gains $\xi_{k\ell}$, $k \neq \ell$:

$$\xi_{k\ell} = \begin{cases} |H_k(\mathrm{i}\,\omega^{(k\ell)})||\zeta_{k\ell}|, & \text{if } J_k \leq J_\ell, \\ \frac{|H_k(0)|}{|H_\ell(0)|} |H_\ell(\mathrm{i}\,\omega^{(k\ell)})||\zeta_{k\ell}|, & \text{if } J_\ell < J_k. \end{cases} \quad (16)$$

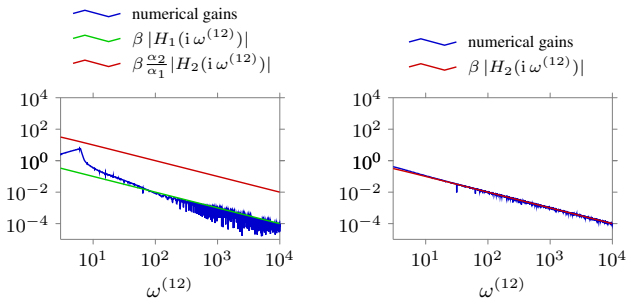

Fig. 6. In this figure we plot the gains ξ_{12} (left panel) and ξ_{21} (right panel) in a logarithmic scale. For this comparison, we select $\beta = \alpha_2 = 1$ and $\alpha_1 = 0.01$; thus, $\zeta_{12} = \zeta_{21} = \beta$, $J_1 = -2\alpha_1$, and $J_2 = -2\alpha_2$. In the left panel, the additional green line represents the approximate gain obtained by truncating the series in (14) after the first term. Notice that, in such a case, the approximation is accurate only for large frequencies $\omega^{(12)}$. The red curve, instead, represent the proposed approximation detailed in (16).

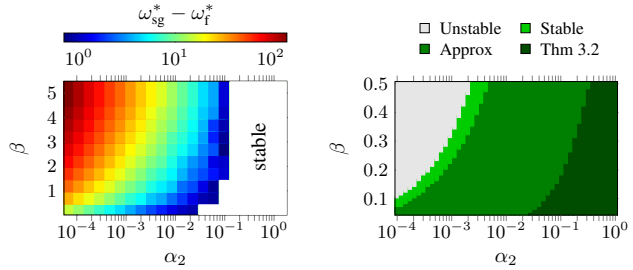

(a) (b)

Fig. 7. The heatmap in Fig. 7(a) represents the error between ω^*_{sg} and ω^*_{f} defined in Example 2. We let $\alpha_1 = \omega_1 = 1$, and β, α_2 vary as indicated. The white area contains stable network realizations predicted by both the Floquet exponents and the condition (11). Fig. 7(b) shows that, for the parameters in Example 1, the approximate stability condition based on Theorem 4.1 and (16) is much tighter than the condition in Theorem 3.2.

Our approximation is validated in Fig. 6 for the network in Fig. 4(a), where it can be seen that, for the considered example, the proposed gains are accurate when $J_\ell > J_k$, and they constitute a reasonable upper bound when $J_\ell < J_k$. Additional studies are required to further validate and support the proposed approximate gains (see also Example 2).

(Approximate stability test) We define the gain matrix $\Xi = [\xi_{k\ell}] \in \mathbb{R}^{m \times m}$, with $\xi_{k\ell} = 0$ if $k = \ell$, and $\xi_{k\ell}$ as in (16) if $k \neq \ell$. Finally, our approximate stability condition for the cluster synchronization manifold consists of applying Theorem 4.1 with the approximate gain matrix Ξ.

Example 2: ***(Tightness of approximate stability condition)*** Consider the network in Example 1. In Fig. 7 we compare the proposed approximate stability condition with the numerical outcomes from Floquet stability theory. In Fig. 7(a) we use the following quantities: ω^*_{sg} is the smallest frequency difference $\omega^{(12)}$ such that condition (11) with gains as in (16) is satisfied, and ω^*_{f} is the smallest frequency difference $\omega^{(12)}$ such that the largest Floquet exponent of (5) is negative. Notice that the approximate condition in (11) closely reproduces the numerical instability-stability transition in a reasonable region of intra- and inter-cluster parameters; namely, for small values of β and $\alpha_2 - \alpha_1$. In Fig. 7(b) we show that our approximate stability condition outperforms the analytical one derived in Theorem 3.2. □

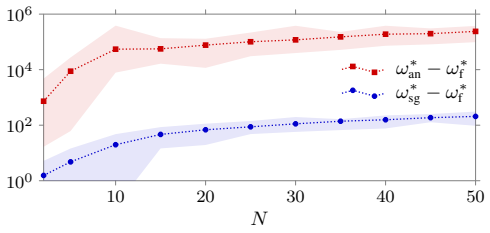

Fig. 8. This figure shows the error between ω^*_{sg} and ω^*_f defined in Example 2 and using the approximate gain matrix (17), as the cardinality of the clusters increases. For each cardinality N, we generate 100 random realizations of the graphs $\mathcal{G}_1$ and $\mathcal{G}_2$ described in Remark 2. The intra-cluster weights of $\mathcal{G}_1$ (resp. $\mathcal{G}_2$) are uniformly distributed in $[0, 1]$ (resp. $[0, 0.01]$), and the inter-cluster weights are uniformly distributed in $[0, 1]$. The dashed blue line represents the mean difference $\omega^*_{sg} - \omega^*_f$ for the approximate gains in (17), and the dashed red line represents the mean difference $\omega^*_{an} - \omega^*_f$ for the analytical test in [20, Theorem 3.5]. The shaded area contains the maximum and minimum values among all realizations.

Remark 2: ***(Extension to clusters with multiple nodes)*** When the clusters contain more than two nodes, a gain matrix similar to (16) can be computed by using a suitable scalar approximation of the transfer matrix $H_k(s) = (sI - J_k)^{-1}$. We propose the following stability test, which relies on using the mean singular value of H_k to compute input-output gains:

$$\xi_{k\ell} = \begin{cases} \nu_{k\ell}\overline{\sigma}(H_k(\mathrm{i}\,\omega^{(k\ell)})), & \text{if } \overline{\lambda}(J_k) \leq \overline{\lambda}(J_\ell), \\ \nu_{k\ell}\frac{\overline{\sigma}(H_k(0))}{\overline{\sigma}(H_\ell(0))}\overline{\sigma}(H_\ell(\mathrm{i}\,\omega^{(k\ell)})), & \text{if } \overline{\lambda}(J_\ell) < \overline{\lambda}(J_k), \end{cases} \tag{17}$$

where $\nu_{k\ell} = \|J_{\text{inter},k\ell}\|$ at time $t = 0$. We validate the approximate stability condition (11) on random networks with $2N$ nodes that are generated as follows. First, we choose two weighted undirected and connected Erdös-Rényi graphs $\mathcal{G}_1$ and $\mathcal{G}_2$ with cardinality N and edge probability $p = 0.5$. To facilitate instability of $\mathcal{S}_\mathcal{P}$ for small natural frequency differences, we select small intra-cluster weights in $\mathcal{G}_2$ (see Fig. 7(a)). Second, we connect $\mathcal{G}_1$ and $\mathcal{G}_2$ to satisfy Assumption (A2). Finally, for each N, we compare the condition (11) with our approximate gains (17) and the condition in [20, Theorem 3.5] with the smallest value of the natural frequency ensuring stability, which is obtained using the Floquet exponents of (5). For different random realizations of $\mathcal{G}_1$ and $\mathcal{G}_2$, Fig. 8 shows that our heuristic test consistently performs better than its analytical counterpart.□

V. Conclusion

In this paper we derive exact and approximate conditions for the local exponential stability of the cluster synchronization manifold in networks of Kuramoto oscillators. Our exact conditions show that the cluster synchronization manifold is stable when the intra-cluster weights are sufficiently larger than the inter-cluster weights, and that stability is also guaranteed when the natural frequencies across different clusters are sufficiently heterogeneous. Our approximate conditions, instead, combine the above independent mechanisms of stability based on the network weights and oscillators' natural frequencies, and are shown to be considerably more accurate than our exact conditions. To the best of our knowledge, the conditions presented in this paper constitute the first explicit and provable results for the stability of the cluster synchronization manifold in general networks of Kuramoto oscillators. Finally, these results are expected to find applicability across different domains, including the characterization and control of abnormal patterns of synchronized neural activity in the human brain, as we are currently investigating.

References

[1] N. E. Leonard, T. Shen, B. Nabet, L. Scardovi, I. D. Couzin, and S. A. Levin. Decision versus compromise for animal groups in motion. *Proc. Natl. Acad. Sci. U.S.A.*, 109(1):227–232, 2012.

[2] F. Dörfler, M. Chertkov, and F. Bullo. Synchronization in complex oscillator networks and smart grids. *Proc. Natl. Acad. Sci. U.S.A.*, 110(6):2005–2010, 2013.

[3] I. Belykh, R. Jeter, and V. Belykh. Foot force models of crowd dynamics on a wobbly bridge. *Sci. Adv.*, 3(11):e1701512, 2017.

[4] F. Dörfler and F. Bullo. Synchronization in complex networks of phase oscillators: A survey. *Automatica*, 50(6):1539–1564, 2014.

[5] F. Sorrentino and E. Ott. Network synchronization of groups. *Physical Review E*, 76(5):056114, 2007.

[6] W. Lu, B. Liu, and T. Chen. Cluster synchronization in networks of coupled nonidentical dynamical systems. *Chaos*, 20(1):013120, 2010.

[7] Z. Aminzare, B. Dey, E. N. Davison, and N. E. Leonard. Cluster synchronization of diffusively-coupled nonlinear systems: A contraction based approach. *Journal of Nonlinear Science*, pages 1–23, 2018.

[8] J. Qin, Q. Ma, H. Gao, Y. Shi, and Y. Kang. On group synchronization for interacting clusters of heterogeneous systems. *IEEE Transactions on Cybernetics*, 47(12):4122–4133, 2017.

[9] C. Hammond, H. Bergman, and P. Brown. Pathological synchronization in Parkinson's disease: networks, models and treatments. *Trends in Neurosciences*, 30(7):357–364, 2007.

[10] K. Lehnertz, S. Bialonski, M.-T. Horstmann, D. Krug, A. Rothkegel, M. Staniek, and T. Wagner. Synchronization phenomena in human epileptic brain networks. *J. Neurosci. Methods*, 183(1):42–48, 2009.

[11] A. Daffertshofer and B. van Wijk. On the influence of amplitude on the connectivity between phases. *Front. Neuroinform.*, 5:6, 2011.

[12] L. M. Pecora, F. Sorrentino, A. M. Hagerstrom, T. E. Murphy, and R. Roy. Cluster synchronization and isolated desynchronization in complex networks with symmetries. *Nature Communications*, 5, 2014.

[13] D. Fiore, G. Russo, and M. di Bernardo. Exploiting nodes symmetries to control synchronization and consensus patterns in multiagent systems. *Control Systems Letters*, 1(2):364–369, 2017.

[14] C. Favaretto, A. Cenedese, and F. Pasqualetti. Cluster synchronization in networks of Kuramoto oscillators. In *IFAC World Congress*, pages 2433–2438, Toulouse, France, July 2017.

[15] Y. Qin, Y. Kawano, and M. Cao. Partial phase cohesiveness in networks of communitinized Kuramoto oscillators. In *European Control Conference*, pages 2028–2033, Limassol, Cyprus, 2018.

[16] M. T. Schaub, N. O'Clery, Y. N. Billeh, J.-C. Delvenne, R. Lambiotte, and M. Barahona. Graph partitions and cluster synchronization in networks of oscillators. *Chaos*, 26(9):094821, 2016.

[17] L. Tiberi, C. Favaretto, M. Innocenti, D. S. Bassett, and F. Pasqualetti. Synchronization patterns in networks of Kuramoto oscillators: A geometric approach for analysis and control. In *IEEE Conf. on Decision and Control*, pages 481–486, Melbourne, Australia, December 2017.

[18] I. V. Belykh, B. N. Brister, and V. N. Belykh. Bistability of patterns of synchrony in Kuramoto oscillators with inertia. *Chaos*, 26(9):094822, 2016.

[19] Y. S. Cho, T. Nishikawa, and A. E. Motter. Stable chimeras and independently synchronizable clusters. *Physical Review Letters*, 119(8):084101, 2017.

[20] T. Menara, G. Baggio, D. S. Bassett, and F. Pasqualetti. Stability conditions for cluster synchronization in networks of heretogeneous Kuramoto oscillators. *IEEE Transactions on Control of Network Systems*, 2019. In press.

[21] A. N. Michel, L. Hou, and D. Liu. *Stability of Dynamical Systems*. Springer, 2008.

[22] H. K. Khalil. *Nonlinear Systems*. Prentice Hall, 3 edition, 2002.

[23] R. A. Horn and C. R. Johnson. *Topics in Matrix Analysis*. Cambridge University Press, 1994.

[24] W. J. Rugh. *Linear System Theory*. Information and System Sciences Series. Prentice Hall, New Jersey, 1993.

[25] S. Dashkovskiy, B. S. Rüffer, and F. R. Wirth. An ISS small gain theorem for general networks. *Mathematics of Control, Signals, and Systems*, 19(2):93–122, 2007.

[26] K. K. Stevens. On the response of linear systems to modulated sinusoidal inputs. *J. Sound Vib.*, 21(3):295–306, 1972.